IEEE Sensors Letters Volume 2(3) (2017)

IEEE Sensors Council

Article Subject (see Index Terms below and write one here) _____

Tactile Sensing System and Convolutional Neural Network for Mechanical Property Classification

V. Oleksyuk[1], N. Rahman[1], and C.-H. Won[1]

[1] *Department of Electrical and Computer Engineering, Temple University, Philadelphia, PA 19122, USA*

Received 1 Nov 2016, revised 25 Nov 2016, accepted 30 Nov 2016, published 5 Dec 2016, current version 15 Dec 2016. (Dates will be inserted by IEEE; "published" is the date the accepted preprint is posted on IEEE Xplore®; "current version" is the date the typeset version is posted on Xplore®).

Abstract—We developed a method to characterize tumors by representing multiple tactile images obtained from Tactile Sensing System. We convert multiple tactile images into a single representative image called Tactile Profile Diagram (TPD). TPD is a pattern image with tactile information about a tumor. TPD is used to estimate the mechanical property of the tumors. We verified the TPD method by classifying tumor phantoms using a Convolutional Neural Network (CNN) with an accuracy of 83% for depth, 78% for stiffness, and 72% for size. We also applied machine learning algorithms for tumor mechanical property classification with the human dataset. CNN classification accuracy of depth, stiffness, and size was 77%, 69%, and 69%, respectively for the human data. Consequently, we conclude that the TPD method is useful for inclusion classification with Tactile Sensing System in breast cancer applications.

Index Terms—breast tumor, convolutional neural network classification, data representation, pattern images, tactile profile diagram, tactile sensors, Tactile Sensing System.

I. INTRODUCTION

Breast masses are the most common breast disease manifestation, where the majority of them are benign [1]. Breast masses can be detected by patients during self-breast examination (SBE), by medical practitioners during a clinical breast examination (CBE), or during a routine screening mammogram [2]. In modern practice, SBE and CBE are not the primary tools for a cancer diagnosis; however, they are very important supplemental screening techniques to mammography, ultrasound, or MRI imaging. CBE is used to identify the lesions and to find 15% of the malignant tumors undetected during mammography [3].

When a tumor is found, physicians complete a detailed assessment of the tumor and the affected breast, evaluate for the possibility of malignancy, and aim to give an accurate diagnosis [1]. To do so, most often, they use mammography and ultrasound imaging to visualize the breast tissues and suspicious masses. Other supplemental tests are available to support the diagnosis [2]. Research shows that cancerous masses tend to be stiffer than benign ones [4],[5], and in some studies, malignant tumors are found to be tenfold stiffer than normal breast tissue through compression experiments [6]. It is also shown that mechanical imaging can classify breast tumors as benign or malignant [7],[8]. Moreover, the size of the detected tumor defines its grade during diagnosis and defines the future treatment plan for the patient [6]. The recent advancement of tactile devices, such as tactile sensors, greatly assists in identifying objects, recognizing objects, and estimating poses in robotics and other applications [9]. We developed Tactile Sensing System and its algorithms to mimic human touch sensation and to non-invasively measure the size and stiffness of embedded tumors [10]-[13]. Our research group first developed Tactile Sensing System to determine the strain and elastic modulus of polymer samples [10]. Further, our research group improved this system [11]-[12]. Building on these works, we convert multiple tactile images into one tactile profile diagram (TPD) that is computationally more efficient as the processing time decreases significantly.

In paper [14], our research group used Tactile Sensing System algorithm to estimate the size and stiffness and then apply machine learning algorithms such as k-nearest neighbor, support vector machine, and Naïve Bayes to classify breast masses as benign or malignant based on the size and stiffness information. Some researchers used the Convolutional Neural Network algorithm to classify benign and malignant tumors based on raw digital mammogram medical images [15], [16] or ultrasound images [17]. Motivated by the fact that CNN is an effective tool for medical image classification, we employed CNN to characterize tumor mechanical properties. More specifically, in our work, we utilize the TPDs and employ CNN models to classify the tumor's mechanical properties such as depth, stiffness, and size of inclusions. In this paper, we classify tumor's mechanical properties and the classification results will be compared with true values for depth, size, and stiffness of human patient data.

II. METHODS

A. Tactile Sensing System and Imaging

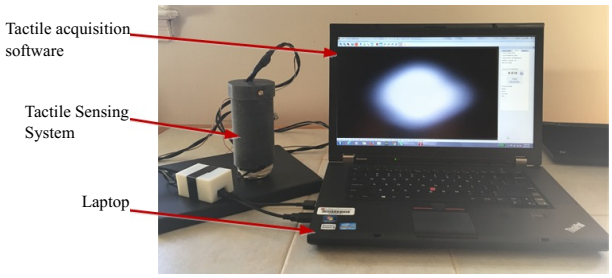

Fig. 1. Tactile sensing system connected to acquisition software

Corresponding author: C.-H. Won (cwon@temple.edu).

Digital Object Identifier: 10.1109/LSEN.XXXX.XXXXXXX (inserted by IEEE).

The Tactile Sensing System exploits the total internal reflection of principle inside the elastic and translucent Polydimethylsiloxane (PDMS) probe as a sensing element to measure tactile properties of tissue inclusions [12], [18], [19]. The built-in lens and CMOS camera (IDS UI-3240CP) capture the reflected rays due to the contact deformation of the probe against a test sample. The applied force starts from 0N and gradually increases to 45N. We acquire a set of images for each compression against the tissue region with inclusion. The size of an individual image is 1024×1280 pixels. The typical number of images in a set for the experiment is 50. The speed of image acquisition is 20 images per second. Finally, acquisition software is used to transfer the data from the camera to the laptop. See. Fig. 1.

B. Tactile Profile Diagram

Here we present a method to construct a Tactile Profile Diagram (TPD), as a representative pattern image of a tactile image set [20]. TPD is a pictorial representation of relative stiffness and size of the inclusion. The range of applied force should be kept the same between different TPDs. See. Fig. 2 for sample TPDs. The method of creating a TPD from multiple tactile images is as follows.

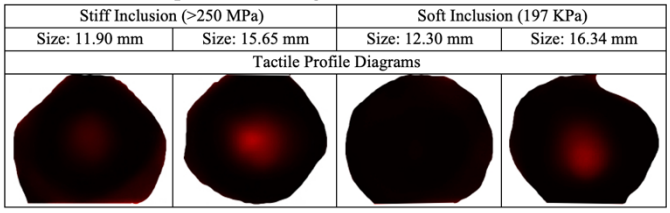

Fig. 2. Sample TPD images

We acquire a set of images with Tactile Sensing System by compressing it on the region with an inclusion. The number of raw tactile images, $I_l(x,y)$, in a set is $l = 1, 2, \ldots, N$. Variables x and y are the horizontal and the vertical coordinates respectively of a pixel within an image I_l. We apply an averaging filter with a non-overlapping sliding window of size $10\ pixels \times 10\ pixels$ to each $I_l(x,y)$, in order to reduce the level of white noise within the images and improve the speed of computation. The pixels values in the created reduced image, $R_l(m,n)$, corresponding to the average values of pixel intensities in the window at each step. The number of reduced images in the set is the same as the number of original images. The size of the reduced images is $103\ pixels(m) \times 128\ pixels(n)$. The reduced images are the more compact copies of tactile raw images. Each tactile image, I_l, has a corresponding compression force value. The $\vec{f_l}$ is the vector of forces of size $N \times 1$. Similar to the pre-load step during Instron tests [21], we select a reference force, f_{ref}, and its corresponding reduced reference image, $R_{ref}(m,n)$, from the set to account for the imperfections at the test tissue surface. Empirically, we chose 5N as f_{ref} and obtain the vector of the change in compression force, as $\overrightarrow{\Delta f_l}$ as,

$$\overrightarrow{\Delta f_l} = \vec{f_l} - f_{ref}. \quad (1)$$

Subsequently, we complete pixel-wise subtraction of the reduced reference image, $R_{ref}(m,n)$, from all reduced images, $R_l(m,n)$, in the set to create an image set ΔR_l, which represents the change in tissue deformation under compression. These images describe the deformation of the silicone probe within Tactile Sensing System.

$$\Delta R_l(m,n) = R_l(m,n) - R_{ref}(m,n). \quad (2)$$

Next, we find the maximum intensity value, ΔR_{max}, present in the ΔR_l image set. Then we subtract each pixel value in ΔR_l images from the ΔR_{max} to get the change of deformation images, ΔW_l, of the tissue with inclusion, and not of the sensing probe's material.

$$\Delta W_l(m,n) = \Delta R_{max} - \Delta R_l(m,n). \quad (3)$$

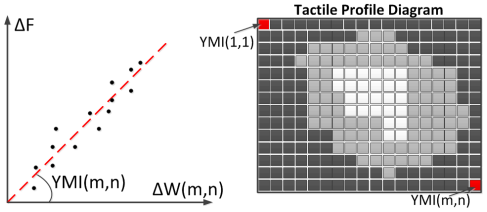

Fig. 3. Young's Modulus Index calculation for a pixel (m,n) and a reconstructed Tactile Profile Diagram

To construct a TPD, we calculate Young's modulus index values, $YMI\ (m,n)$ which is the stiffness estimation parameter, for each pixel location in ΔW_l (Fig. 3). We mimic the definition of Young's modulus and calculate YMI in a pixel location (m,n) as a slope of the compression force over an area (the compression change $\overrightarrow{\Delta f_l}$) vs. the deformation change due to the compression (the change in deformation ΔW_l for the tissue with inclusion). To calculate the slope in each pixel location (m,n), N data points will be used from a tactile image set. A Tactile Profile Diagram (TPD) is obtained by plotting $YMI\ (m,n)$ for $m = 1$ to 103 and $n = 1$ to 128 (Fig. 3). If $\overrightarrow{\Delta f_l}$ is divided by the contact area and ΔW_l is correlated with the strain, then YMI is related to the young's modulus of the tissue.

C. Tactile Profile Diagram Classification

We classified Tactile Profile Diagrams using CNN. See. Fig. 4. Convolutional Neural Network (CNN) proved to work well with image classification tasks [22],[23]. CNN includes a set of convolutional layers with corresponding activation functions, max-pooling layers, and fully connected layers with a Softmax function for the final classification decision.

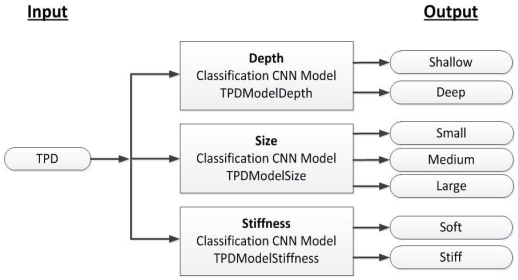

Fig. 4. TPD classification method

We employed three CNN models to classify tactile profile diagrams and to characterize the depth, stiffness, and size of imaged tumors. The depth classification model is shown in Fig. 5 where we classified tumors as deep or shallow. Similarly, we classified small, medium, or large tumors employing the size model, and stiff or soft tumors from the stiffness model. We designed CNN sequential models without a feedback loop, with three convolution layers, three Max pooling layers, and activation functions for the feature learning part. We employed Adamax optimizer, and accuracy as the metric for the model performance evaluation during training. The model's training and validation data is developed from tactile phantom imaging data

combined into the Tactile Profile Diagrams dataset for classification. With the sufficient training data and the modified final layer, the model can output multiple classes if required by the application.

Depth, Size, and Stiffness Classification

The depth and stiffness TPD models are designed as 2 class and size TPD model is designed as 3 class classifiers to distinguish the classes. Fig. 5 shows the structure of the depth classification model. The classification part of all the models includes four dense layers with ReLU and ELU activation functions and Dropout layers of 0.3 and 0.2. The final fully connected layer has a Softmax activation function. In depth, size, and stiffness model there are two, three, and two nodes, corresponding to the shallow or deep classes, small or medium or large classes, and soft or stiffness classes respectively.

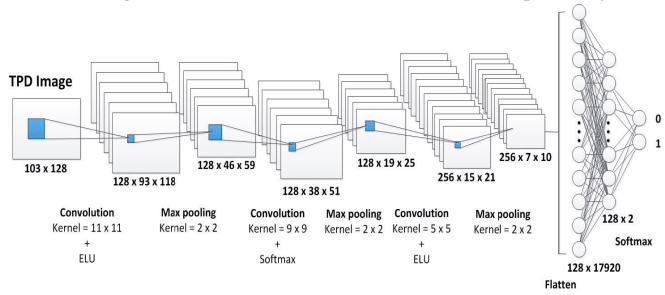

Fig. 5. CNN model for tumor depth classification

III. EXPERIMENTS AND RESULTS

A. Phantom and setup

The tactile breast tissue phantom is composed of multiple layers. The base material of the tissue layers is PDMS due to its safety and easiness to use, adjustable stiffness, and high tolerance to heat and mechanical compressions. PDMS is commercially available silicone rubber and composed of two materials: Base agent (A) and Curing Agent (B). Two components A and B were mixed in different ratio by weight. These ratios are given in Fig. 6. We developed four types of tissue layers using PDMS: base, intermediate, depth, and skin layers. Fig. 6 shows the schematics of the phantom and its layers. The description of each layer is also provided in the figure. The spherical tumors are manually cut out of cured PDMS with a range of stiffness to mimic different tumor sizes and stiffness characteristics.

B. Classification: Depth, Size, and Stiffness

Depth Model: To train the Depth model we used samples of varying sizes (10 mm, 12 mm, 14 mm, 16 mm, 18 mm) and stiffness (from 130 kPa to > 250 MPa). We included a shallow tumor subset: depths of 0 mm, 2 mm, and 4 mm, and a deep tumor subset: depths of 6 mm, 8 mm, and 10 mm. During the model development, the data division was 80% for training and 20% for validation. The model was trained on 6768 TPDs and validated on 1692 TPDs. The validation accuracy was 96%.

Size Model: During training the Size model we included varying depths (0 mm, 2 mm, 4 mm, 6 mm, 8 mm, and 10 mm) and stiffness (130 kPa − 250 MPa). The sizes were 10 mm, 12 mm, 14 mm, 16 mm, 18 mm, and 23 mm. We divided the dataset into three classes depending on the size of the tumor: small (10 mm and 12 mm), medium (14 mm and 16 mm), and large (18 mm and 23 mm). The model was trained on 6789 TPDs and validated on 1696 TPDs. The validation accuracy was 96%.

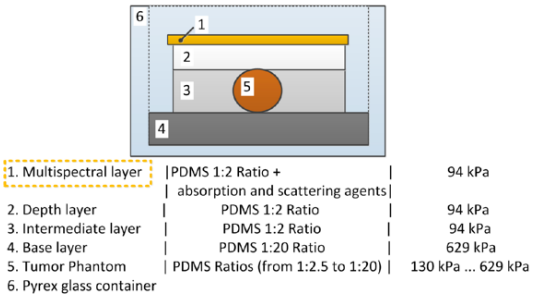

Fig. 6. Schematics diagram of phantom and its layers

Table 1. CNN classification results for the phantom data

Sample	Depth		Stiffness		Size	
	CNN Class	CNN Class (Prob± STD)	CNN Class	CNN Class (Prob± STD)	CNN Class	CNN Class (Prob± STD)
1	Shallow	0.73±0.00	Stiff	0.73±0.00	Medium	0.32±0.13
2	Shallow	0.57±0.19	Stiff	0.58±0.27	Small	0.46±0.21
3	Shallow	0.72±0.01	Soft	0.73±0.01	Small	0.57±0.01
4	Shallow	0.70±0.06	Stiff	0.59±0.25	Medium	0.58±0.01
5	Shallow	0.62±0.2	Stiff	0.64±0.16	Medium	0.57±0.01
6	Deep	0.35±0.12	Stiff	0.47±0.21	Small	0.28±0.06
7	Shallow	0.73±0.00	Stiff	0.73±0.00	Large	0.58±0.00
8	Deep	0.37±0.15	Stiff	0.73±0.00	Large	0.58±0.01
9	Shallow	0.59±0.10	Soft	0.54±0.24	Medium	0.30±0.14
1	Deep	0.73±0.00	Soft	0.44±0.25	Small	0.37±0.16
2	Deep	0.72±0.00	Soft	0.27±0.01	Small	0.53±0.02
3	Deep	0.70±0.02	Soft	0.68±0.08	Small	0.48±0.08
4	Deep	0.65±0.11	Stiff	0.73±0.00	Medium	0.56±0.02
5	Deep	0.62±0.19	Soft	0.49±0.23	Medium	0.54±0.03
6	Deep	0.68±0.08	Soft	0.73±0.00	Small	0.31±0.09
7	Shallow	0.27±0.01	Stiff	0.73±0.00	Large	0.58±0.00
8	Deep	0.69±0.06	Stiff	0.73±0.00	Large	0.58±0.01
9	Deep	0.73±0.00	Soft	0.55±0.25	Small	0.22±0.01
Accuracy		0.83		0.78		0.72

Stiffness Model: The Stiffness model was trained on varying sizes and depths samples same as the depth model. The stiffness of embedded tumors ranged from 130 kPa to more than 250 MPa. The soft tumors subset included 130 kPa to 316 kPa samples and the stiff tumors subset included tumors from 376 kPa to more than 250 MPa samples. The model was trained on 6788 TPDs and validated on 1697 TPDs. The validation accuracy was 91%.

C. Classification: Human and Phantom Data

Phantom Data: Results from TPD classification are presented in Table 1. In the table, the green shaded rows indicate deep tumors, the light brown rows indicate stiff tumors, and light and darker blue rows correspond to medium and large size tumors, respectively. classification accuracy for depth, stiffness, and size for the test set are 83% 78%, and 72%, respectively. See Table 1. The misclassified cases are shown in red. The size accuracy is low because the time difference between the calibration and measurement times of the samples for the TPD size model was relatively large and the PDMS sensing element slightly changed its properties.

Table 2. CNN classification results for the human data

Patient	Depth		Stiffness		Size	
	US Est. Class	CNN Class	Doctor Est. Class	CNN Class	US Est. Class	CNN Class
1	Shallow	Deep	Stiff	Stiff	Small	Large
2	Shallow	Deep	Stiff	Soft	Large	Small
3	Shallow	Shallow	Stiff	Stiff	Large	Large
4	Shallow	Shallow	Soft	Soft	Medium	Medium
5	Shallow	Shallow	Soft	Stiff	Large	Small
6	Shallow	Shallow	Stiff	Stiff	Large	Large
7	Shallow	Deep	Soft	Soft	Large	Large
8	Shallow	Shallow	Stiff	Stiff	Medium	Medium
9	Shallow	Shallow	Soft	Stiff	Medium	Large
10	Deep	Deep	Soft	Soft	Large	Large
11	Deep	Deep	Soft	Stiff	Small	Small
12	Deep	Deep	Soft	Soft	Large	Large
13	Shallow	Shallow	Stiff	Stiff	Small	Small
Accuracy		0.77		0.69		0.69

Human Data: We used 13 human datasets to test the developed methods. CNN classification accuracy for depth, stiffness, and size were 77%, 69%, and 69%, respectively. Results are presented in Table 2. The low size estimation error can be again attributed to the differences in PDMS probe condition between the imaging experiments for the model development and the time of human data acquisition.

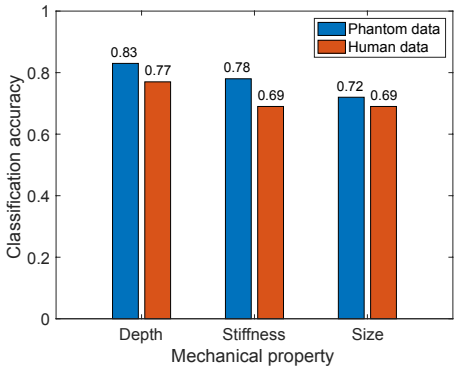

Fig. 7. Visualization of phantom and human data

Fig. 7 represents the classification accuracy of the phantom and human data. It seems that phantom data has slightly better classification results compared to human data as the calibration of our Tactile Sensing System is based on phantom. But still, human data has given consistent and satisfactory classification results with our developed model.

IV. CONCLUSION

We utilized Tactile Profile Diagram (TPD) to obtain the mechanical properties of tumors. There are many advantages of using TPDs over the use of raw tactile image sets. The tactile property information in TPD is visual, condensed, and easier to interpret. Each pixel in a TPD carries dynamic tactile information of the tested region under the range of compression forces. While creating a TPD decreases the spatial resolution of tactile images, most of the spatial information is preserved, and less storage is required for TPDs than for sets of multiple tactile images. The spatial resolution of TPDs can be increased to match the resolution of raw tactile images; however, that will come at the expense of storage and computation speed. Finally, the TPD method opens the possibility of applying deep learning techniques, such as Convolutional Neural Networks (CNN), for malignant/benign classification in clinical breast cancer applications. We used 13 human datasets to test the developed classification methods. For the human data set, CNN classification accuracy for depth, stiffness, and size were 77%, 69%, and 69% respectively. So, we conclude that tumor's mechanical properties are accurately classified using Tactile Sensing System. This system can be used in breast tumor characterization application.

ACKNOWLEDGMENT

The authors would like to thank Arpita Das for her assistance in data organization. This work was supported in part by the National Science Foundation's ECCS-2114675.

REFERENCES

[1] T.M.J. R. Harris, J. Pine, Jonathan W., J. Goolsby, E. Moyer, B. Dougherty, Diseases of the Breast, 5th ed. Philadelphia: Wolters Kluwer, 2014.
[2] J. Hellawell, Breast Diseases. 2008.
[3] A. Aydiner, A. Igci, and A. Soran, Breast Disease. Diagnosis and Pathology. Springer, 2017.
[4] T. A. Krouskop, T. M. Wheeler, F. Kallel, B. S. Garra, and T. Hall, "Elastic moduli of breast and prostate tissues under compression.," Ultrason. Imaging, vol. 20, no. 4, pp. 260–274, 1998
[5] P. S. Wellman, "Tactile Imaging," Harvard University, Cambridge, MA, 1999.
[6] B. D. Price, a P. Gibson, L. T. Tan, and G. J. Royle, "An elastically compressible phantom material with mechanical and x-ray attenuation properties equivalent to breast tissue.," Phys. Med. Biol., vol. 55, no. 4, pp. 1177–1188, 2010.
[7] V. Egorov, T. Kearney, S.B. Pollak, C. Rohatgi, N. Sarvazyan, S. Airapetian, S. Browning, and A. Sarvazyan, "Differentiation of benign and malignant breast lesions by mechanical imaging," Med. Imaging, IEEE Trans., vol. 118, no. 1, pp. 67–80, Nov. 2009.
[8] V. Egorov and A. P. Sarvazyan, "Mechanical imaging of the breast," IEEE Trans. Med. Imaging, vol. 27, no. 9, pp. 1275–1287, 2008.
[9] Luo, S., Bimbo, J., Dahiya, R., & Liu, H. (2017). Robotic tactile perception of object properties: A review. Mechatronics, 48, 54-67.
[10] J. Lee and C. Won, "High Resolution Tactile Imaging Sensor Using Total Internal Reflection and Non-rigid Pattern Matching Algorithm," IEEE Sens. J., vol. 11, no. 9, pp. 2084–2093, Sep. 2011.
[11] F. Saleheen and C.-H. Won, "Dynamic Positioning Sensing System for Estimating Size, Depth and Elastic Modulus of Embedded Object," in Proc. IEEE Sensors, 2015, pp. 1–6.
[12] V. Oleksyuk, R. Rajan, F. Saleheen, D. F. Caroline, S. Pascarella, and C. Won, "Risk Score Based Pre-screening of Breast Tumor Using Compression Induced Sensing System," IEEE Sens. J., 2018.
[13] N. Rahman, C. H. Won, "Identifying Benign and Malignant Breast Tumor Using Vibro-acoustic Tactile Imaging Sensor," IEEE Sensors (pp. 1-4), 2022.
[14] V. Oleksyuk, F. Saleheen, D. F. Caroline, S. Pascarella, C. Won, "Classification of breast masses using Tactile Imaging System and machine learning algorithms," IEEE Signal Processing in Medicine and Biology Symposium (SPMB), 2016.
[15] F. F. Ting, Y. J. Tan, K. S. Sim, "Convolutional neural network improvement for breast cancer classification", Expert Systems with Applications, 120, 103-115, 2019.
[16] H. Chougrad, H. Zouaki, O. Alheyane, "Deep convolutional neural networks for breast cancer screening", Computer methods and programs in biomedicine, 157, 19-30, 2018.
[17] J. Y. Chiao, K. Y. Chen, K. Y. K. Liao, P. H. Hsieh, G. Zhang, T. C. Huang, "Detection and classification the breast tumors using mask R-CNN on sonograms", Medicine, 98(19), 2019.
[18] J.-H. Lee and C. H. Won, "High Resolution Tactile Imaging Sensor using Total Internal Reflection and Non-Rigid Pattern Matching," IEEE Sens. J., vol. 11, no. 9, pp. 2084–2093, 2011.
[19] J.-H. Lee and C.-H. Won, "The tactile sensation imaging system for embedded lesion characterization," IEEE J. Biomed. Heal. Informatics, vol. 17, no. 2, pp. 452–458, 2013.
[20] M. D. Riley, Speech Time-Frequency Represenations. Kluwer Academic Publishers, 1989.
[21] E. Mangano, "Preloading, and How It Affects Your Mechanical Test".
[22] I. Goodfellow, Y. Bengio, and A. Courville, Deep Learning. Cambridge, Mass: MIT Press, 2017.
[23] A. Geron, Hands-on machine learning with Scikit-Learn and TensorFlow concepts, tools, and techniques to build intelligent systems, 2nd Edition. O'Reilly Media Inc., 2019.